

658° C is about 0.000 27 Å in the *a* parameter and about 0.001 03 Å in the *c* parameter.

The temperature dependence of the coefficients of thermal expansion  $\alpha_{\parallel}$  along the *c*-axis and  $\alpha_{\perp}$  at right angles to the *c*-axis are represented by the following equations:

$$\alpha_{\parallel} = 6.221 \times 10^{-6} + 4.876 \times 10^{-9} T - 2.226 \times 10^{-13} T^2 \quad (1)$$

$$\alpha_{\perp} = 5.583 \times 10^{-6} + 7.181 \times 10^{-9} T - 7.023 \times 10^{-12} T^2 \quad (2)$$

where *T* is the temperature in °C.

The observed coefficients of expansion at different temperatures are given in Table II along with the calculated values obtained from Equations 1 and 2.

TABLE II Coefficients of thermal expansion of InBO<sub>3</sub> at different temperatures

Temperature (°C)	$\alpha_{\parallel} \times 10^6$		$\alpha_{\perp} \times 10^6$	
	Obs.	Calc.	Obs.	Calc.
50	6.53	6.46	5.70	5.93
90	6.69	6.66	6.22	6.18
130	6.77	6.85	6.47	6.41
170	6.85	7.04	6.73	6.61
210	7.26	7.24	6.84	6.79
250	7.58	7.43	7.15	6.95
290	7.74	7.62	7.15	7.08
330	7.74	7.80	7.15	7.19
370	7.98	7.99	7.26	7.29
410	8.07	8.18	7.36	7.35
450	8.47	8.37	7.04	7.40
490	8.47	8.55	7.36	7.42
530	8.87	8.74	7.36	7.43
570	8.87	8.92	7.51	7.40
610	9.11	9.11	7.51	7.36

In Table III, the room temperature lattice constants obtained in the present study are compared with those available in the literature. The value of the *c* parameter obtained in the present study is slightly higher than those reported by the

TABLE III Lattice parameters of InBO<sub>3</sub> at room temperature

Reference	<i>a</i> (Å)	<i>c</i> (Å)
[7]	4.823	15.456
[8]	4.766 ± 0.01	15.455 ± 0.04
Present study	4.8224 ± 0.0002	15.4891 ± 0.001

other investigators. In the case of *a*, the value reported by Goldschmidt and Hauptmann [8] is lower than the other values.

### Acknowledgement

The authors wish to thank the Council of Scientific and Industrial Research, New Delhi for the sanction of a scheme.

### References

1. K. V. KRISHNA RAO, S. V. NAGENDER NAIDU and K. SATYANARAYANA MURTHY, *J. Phys. Chem. Solids* **29** (1968) 245.
2. K. V. KRISHNA RAO and K. SATYANARAYANA MURTHY, *Curr. Sci.* **38** (1969) 162.
3. *Idem*, *J. Mater. Sci.* **5** (1970) 82.
4. *Idem*, *ibid* **9** (1974) 1196.
5. *Idem*, *J. Phys. Chem. Solids* **31** (1970) 887.
6. *Idem*, *Ind. J. Pure and Appl. Phys.* **11** (1973) 230.
7. ERNEST M. LEVIN, ROBERT S. ROTH and JERRY B. MARTIN, *Amer. Min.* **46** (1961) 1030.
8. V. M. GOLDSCHMIDT and H. HAUPTMANN, *Nachr. Ges. Wiss. Gott. Math-phys. kl.* (1931-32) 53.

Received 25 November 1976  
and accepted 4 January 1977

K. SATYANARAYANA MURTHY  
Department of Physics,  
Nizam College,  
Hyderabad-5000017, India

K. V. KRISHNA RAO  
Department of Physics,  
Osmania University,  
Hyderabad-5000017, India

### Fracture surface energies of high explosives PETN and RDX

PETN (pentaerythritol tetranitrate) and RDX (cyclotrimethylene trinitramine) are important solid high explosives which are used extensively in industrial and military applications. Explosion

in these materials can be initiated by mechanical impact and shock. Although a considerable amount of work has been done on their sensitiveness, the exact role of their mechanical properties is not understood. It has, however, been pointed out by some workers that the localization of energy by plastic flow can play an important role in the

initiation of reaction [1–3]. It is also likely that mechanical break-up in these materials can alter their explosive behaviour, (i) by increasing surface area and thus enhancing their reactivity [4] and (ii) by facilitating propagation of reaction [5], especially during the early stages of its growth. It is clear that a knowledge of the failure behaviour of these materials is desirable.

One method of characterizing the susceptibility to fracture of a material is through its fracture toughness, which is equal to  $2\gamma$  where  $\gamma$  is the energy required to create a unit area of surface. In the present study we have used a micro-indentation fracture mechanics approach to determine the surface energy of PETN and RDX single crystals. A particular advantage of indentation is that it allows fracture toughness to be evaluated from relatively small samples.

The method involves indenting the test material with a Vickers diamond pyramid. At small loads, indentations in a material can usually be formed without any associated cracking, even in brittle solids; however, at relatively high loads circular cracks develop beneath the indenter and, with increasing load, extend to the surface, giving traces of surface cracks. The fracture mechanics of such indentation cracks have recently been developed by Lawn and Fuller [6]. They show that the load on the indenter,  $P$ , and the length,  $C$ , of the surface crack are related by

$$\frac{\chi P}{C^{3/2}} = \left( \frac{2\gamma E}{1-\nu^2} \right)^{1/2} \quad (\text{for plane strain conditions}) \quad (1)$$

where  $E$  is the Young's modulus,  $\nu$  is Poisson's ratio and  $\chi$  is a constant dependent upon the geometry of the indenter, the Poisson's ratio of the indented material, and the coefficient of friction between the indenter and the indented material. The values of the coefficient of friction for crystals of PETN and RDX rubbing against a hard surface (for example, glass) are 0.4 and 0.35 [7] respectively. The constants  $\chi$  for PETN and RDX with a Vickers indenter are, therefore,  $\sim 0.17$  and  $\sim 0.15$  respectively. The value of Poisson's ratio  $\nu$  is 0.22 for PETN [8], and it has been assumed to be the same for RDX.

Good quality single crystals of PETN and RDX of dimensions 10 mm  $\times$  5 mm  $\times$  2 mm were grown in the laboratory; PETN crystals were recrystal-

lized from solution in acetone whereas RDX were obtained from solution in dimethylformamide. Indentations were made on a flat face of a crystal with a Vickers diamond indenter using a Leitz microindentation hardness machine. The indenter load was varied in the range 0.15 to 0.7 N. It was found that cracks appeared in both PETN and RDX crystals, even for the smallest load. The extent of the surface crack was measured for each load with an optical microscope using transmitted light. Indentations in both PETN and RDX crystals were made so that the cracks were formed on well-defined cleavage planes. This allowed a study of the anisotropy for various cleavage planes in the crystal. The cleavage plane in PETN is  $\{110\}$ . The

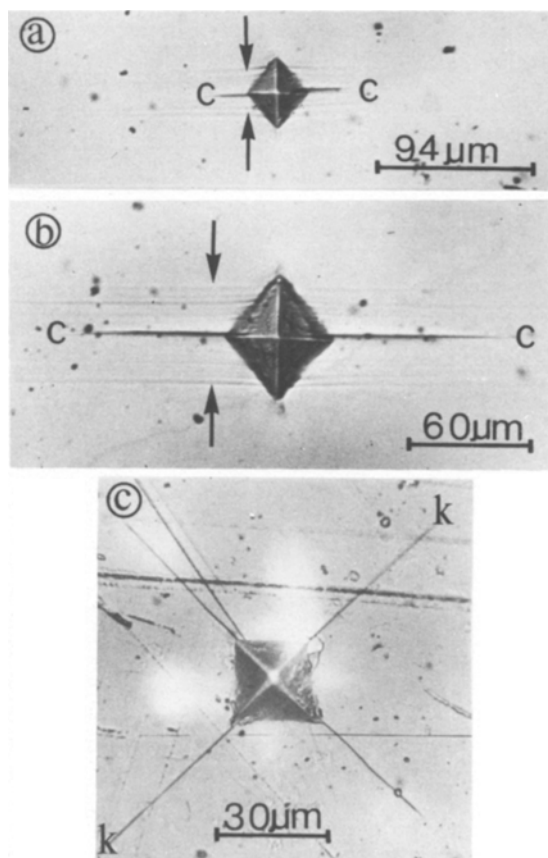


Figure 1 (a) and (b) Vickers hardness indentations in PETN for indenter loads of 0.15 and 0.5 N respectively. The traces of slip lines (arrowed) are parallel to the trace of surface crack, CC, and extend appreciable distances from the indentation. (c): Vickers hardness indentation in RDX for indenter load of 0.5 N. Trace of surface flaw marked KK, is normal to growth features (not shown).

cleavage planes in RDX were found to be parallel and perpendicular to the extended diamond-shaped growth features characteristic of RDX crystals grown in the manner mentioned earlier. Fig. 1 shows micrographs of typical indentations in crystals of PETN and RDX; traces of the slip lines around the indentation in the PETN crystal are indicated by the arrows. Plots of  $P$  against  $C^{3/2}$  for both types of crystal are shown in fig. 2a and b. Knowing the value of  $E$  for PETN [8] ( $E = 1.37 \times 10^{10} \text{ N m}^{-2}$ ) and the slope of the straight line, we can obtain the surface energy from Equation 1. For PETN the fracture surface energy is  $0.11 \text{ J m}^{-2}$ .

The value of the Young's modulus  $E$  for RDX is not known. However, a reasonable estimate can be made from the knowledge that in materials of similar bonding (PETN and RDX are both van der Waals solids) the ratio of the Vickers hardness number and the Young's modulus is approximately constant. The values of the Vickers hardness number for PETN and RDX are 17.9 and  $24.1 \text{ kg mm}^{-2}$  respectively, so the value of  $E$  for RDX can be estimated as  $1.84 \times 10^{10} \text{ N m}^{-2}$ , and the fracture surface energies of the two cleavage planes as  $0.11 \text{ J m}^{-2}$ , and  $0.07 \text{ J m}^{-2}$  respectively

for the cleavage planes parallel and perpendicular to the growth features. These values are of the same order of magnitude as those found for other organic solids using different techniques [9]. When compared with values for crystals with other forms of bonding (see, for example, [10]) it is clear that PETN and RDX are relatively weak and therefore very susceptible to fracture. It should also be emphasized that gross plastic flow associated with the cracks is likely to give an *overestimate* of the surface energy. It can be seen from Fig. 1a and b that extensive plastic flow was observed in PETN, and therefore the true value of its surface energy may be somewhat lower than  $0.11 \text{ J m}^{-2}$ .

The fracture surface energy of explosive samples is a reasonably good indicator of their structural integrity characteristics. It has been found [11] that some loss of structural homogeneity occurs in propellants in rocket motors and explosive charges in shells during launching. Although there may be a number of factors contributing towards this phenomenon, we believe that the low surface energy of many explosive materials is important. Thus, by suitably controlling the surface energy of explosive composites (for example, by using additives), their performance may be considerably improved. An

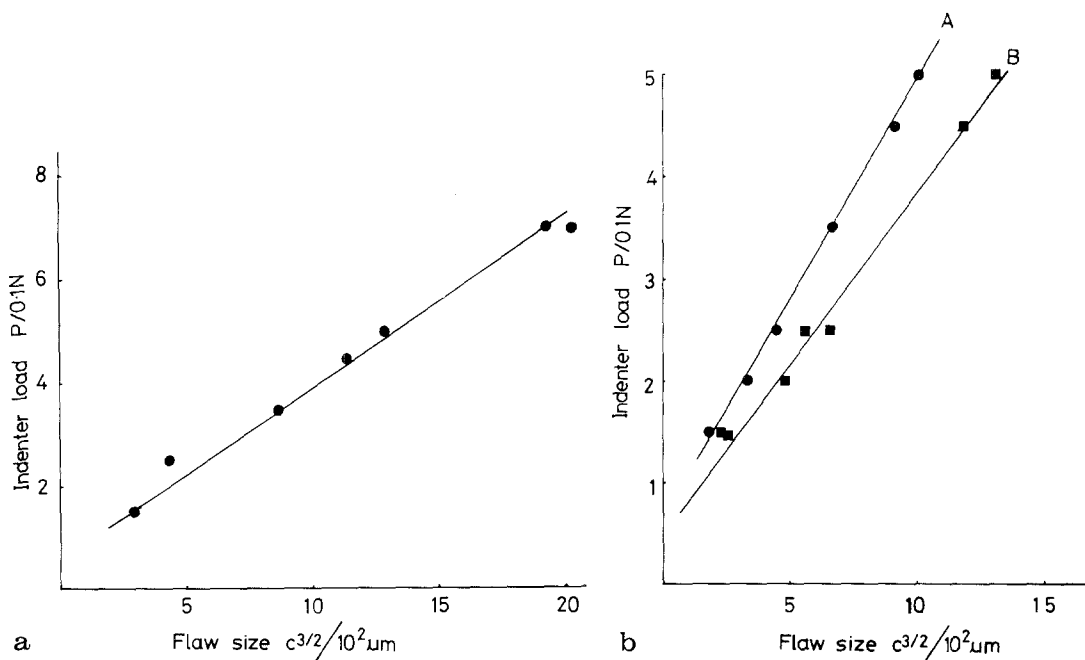


Figure 2 (a) The variation of flaw size  $C$  (half the surface trace) with indenter load  $P$  for PETN. (b) The variation of flaw size with indenter load for RDX. The lines A and B are for the two cleavage planes, parallel and normal to the diamond-shaped growth features.

important feature of the present paper is that it has demonstrated that a simple technique such as indentation can be effective in determining both the plastic flow properties of a material (from the hardness value) and the fracture surface energy. This is particularly useful with explosive materials where samples cannot conveniently be obtained for more conventional fracture mechanics tests.

### Acknowledgements

We thank Dr J.E. Field for his encouragement, and the Procurement Executive, Ministry of Defence.

### References

1. G. T. AFANAS'EV and V. K. BOBOLEV, "Initiation of solid explosives by impact" (Israel Program for Scientific Translations, Jerusalem, 1971) Translation.
2. S. N. HEAVENS and J. E. FIELD, *Proc. Roy. Soc. Lond.* **A338** (1974) 77.
3. R. E. WINTER and J. E. FIELD, *ibid* **A343** (1975) 399.

4. R. F. WALKER, N. GANE and F. P. BOWDEN, *ibid* **A294** (1966) 417.
5. F. P. BOWDEN and A. D. YOFFE, "Fast Reactions in Solids" (Butterworths, London, 1958) Ch. IX.
6. B. R. LAWN and E. R. FULLER, *J. Mater. Sci.* **10** (1975) 2016.
7. J. K. A. AMUZU, B. J. BRISCOE and M. M. CHAUDHRI, *J. Phys. D.* **9** (1976) 133.
8. P. M. HALLECK and J. WACKERLE, *J. Appl. Phys.* **47** (1976) 976.
9. D. TABOR, "Surface Physics of Materials", Vol. II (Academic Press, London, 1975) Ch. 10.
10. J. J. GILMAN, *J. Appl. Phys.* **31** (1960) 2208.
11. D. L. SMITH and B. W. Thorpe, *J. Mater. Sci.* **8** (1973) 757.

Received 17 November  
and accepted 16 December 1976

J. T. HAGAN  
M. M. CHAUDHRI  
Cavendish Laboratory,  
Madingley Road,  
Cambridge, UK

### The dependence of the fracture stress of beta-alumina on microstructural defects

The use of sodium beta-alumina as a solid electrolyte and separator in the sodium-sulphur battery is now well established [1-5]. The majority of cell designs use polycrystalline beta-alumina in the form of a thin-walled tube although flat plate designs have been considered [6, 7]. In either case, the electrolyte contributes substantially to the overall cell impedance and in order to minimize this, the electrolyte should be a thin membrane with a low intrinsic ionic resistivity. At the same time, the membrane must have adequate mechanical strength to allow construction and operation of the cell without premature ceramic failure.

The fracture strength,  $\sigma_f$ , of ceramic materials is largely governed by the stress necessary to propagate small microstructural flaws according to the familiar Griffith relationship,

$$\sigma_f = (2E\gamma_i/\pi c)^{1/2} \quad (1)$$

where  $\gamma_i$  is the fracture initiation energy,  $c$  is half the length of an elliptical flaw and  $E$  is Young's modulus. Experimental data on the tensile strength of ceramics in short-term tests can be conveniently

analysed statistically using Weibull's weakest link concept [8]. The probability of survival,  $P$ , is given by,

$$P = \exp[-D(\sigma_f - \sigma_u/\sigma_0)^m], \quad (2)$$

where  $D$  is the stressed volume,  $\sigma_u$  the zero probability stress,  $\sigma_0$  a normalizing constant and  $m$  the Weibull modulus. Consequently,

$$\ln \ln 1/P = m \ln(\sigma_f - \sigma_u) - m \ln \sigma_0 + \ln D, \quad (3)$$

and so a plot of  $\ln \ln 1/P$  against  $\ln \sigma_f$  with  $\sigma_0$  set equal to zero yields a straight line with a slope equal to the Weibull modulus. In this note we report strength measurements of beta-alumina with two extremes of sample size and describe a preliminary study of the types of microstructural defect responsible for weakening the material.

The beta-alumina used in this work was prepared as closed-ended tubes by direct mixing of the constituent oxide powders together with small amounts of  $\text{Li}_2\text{O}$  and  $\text{MgO}$  to promote the formation of the more conductive  $\beta''$ -phase. Green shapes with uniform density and close dimensional tolerances were prepared by isostatic pressing and these were rapidly sintered at temperatures between